

## MIT Open Access Articles

*Recent increases in the atmospheric growth rate and emissions of HFC-23 (CHF<sub>3</sub>) and the link to HCFC-22 (CHClF<sub>2</sub>) production*

The MIT Faculty has made this article openly available. **Please share** how this access benefits you. Your story matters.

**Citation:** Simmonds, Peter G. et al. "Recent increases in the atmospheric growth rate and emissions of HFC-23 (CHF<sub>3</sub>) and the link to HCFC-22 (CHClF<sub>2</sub>) production." Atmospheric Chemistry and Physics 18, 6 (March 2018): 4153–4169 © 2018 Author(s)

**As Published:** <http://dx.doi.org/10.5194/ACP-18-4153-2018>

**Publisher:** Copernicus GmbH

**Persistent URL:** <http://hdl.handle.net/1721.1/117597>

**Version:** Final published version: final published article, as it appeared in a journal, conference proceedings, or other formally published context

**Terms of use:** Creative Commons Attribution 4.0 International License





## Recent increases in the atmospheric growth rate and emissions of HFC-23 (CHF<sub>3</sub>) and the link to HCFC-22 (CHClF<sub>2</sub>) production

Peter G. Simmonds<sup>1</sup>, Matthew Rigby<sup>1</sup>, Archie McCulloch<sup>1</sup>, Martin K. Vollmer<sup>2</sup>, Stephan Henne<sup>2</sup>, Jens Mühle<sup>3</sup>, Simon O'Doherty<sup>1</sup>, Alistair J. Manning<sup>4</sup>, Paul B. Krummel<sup>5</sup>, Paul J. Fraser<sup>5</sup>, Dickon Young<sup>1</sup>, Ray F. Weiss<sup>3</sup>, Peter K. Salameh<sup>3</sup>, Christina M. Harth<sup>3</sup>, Stefan Reimann<sup>2</sup>, Cathy M. Trudinger<sup>5</sup>, L. Paul Steele<sup>5</sup>, Ray H. J. Wang<sup>6</sup>, Diane J. Ivy<sup>7</sup>, Ronald G. Prinn<sup>7</sup>, Blagoj Mitrevski<sup>5</sup>, and David M. Etheridge<sup>5</sup>

<sup>1</sup>Atmospheric Chemistry Research Group, University of Bristol, Bristol, UK

<sup>2</sup>Swiss Federal Laboratories for Materials Science and Technology, Laboratory for Air Pollution and Environmental Technology (Empa), Dübendorf, Switzerland

<sup>3</sup>Scripps Institution of Oceanography (SIO), University of California at San Diego, La Jolla, California, USA

<sup>4</sup>Met Office Hadley Centre, Exeter, UK

<sup>5</sup>Climate Science Centre, Commonwealth Scientific and Industrial Research Organisation (CSIRO) Oceans and Atmosphere, Aspendale, Victoria, Australia

<sup>6</sup>School of Earth, and Atmospheric Sciences, Georgia Institute of Technology, Atlanta, Georgia, USA

<sup>7</sup>Center for Global Change Science, Massachusetts Institute of Technology, Cambridge, Massachusetts, USA

**Correspondence:** Peter G. Simmonds (petergsimmonds@aol.com)

Received: 6 October 2017 – Discussion started: 12 October 2017

Revised: 2 February 2018 – Accepted: 11 February 2018 – Published: 26 March 2018

**Abstract.** High frequency measurements of trifluoromethane (HFC-23, CHF<sub>3</sub>), a potent hydrofluorocarbon greenhouse gas, largely emitted to the atmosphere as a by-product of the production of the hydrochlorofluorocarbon HCFC-22 (CHClF<sub>2</sub>), at five core stations of the Advanced Global Atmospheric Gases Experiment (AGAGE) network, combined with measurements on firn air, old Northern Hemisphere air samples and Cape Grim Air Archive (CGAA) air samples, are used to explore the current and historic changes in the atmospheric abundance of HFC-23. These measurements are used in combination with the AGAGE 2-D atmospheric 12-box model and a Bayesian inversion methodology to determine model atmospheric mole fractions and the history of global HFC-23 emissions. The global modelled annual mole fraction of HFC-23 in the background atmosphere was  $28.9 \pm 0.6$  pmol mol<sup>-1</sup> at the end of 2016, representing a 28 % increase from  $22.6 \pm 0.4$  pmol mol<sup>-1</sup> in 2009. Over the same time frame, the modelled mole fraction of HCFC-22 increased by 19 % from  $199 \pm 2$  to  $237 \pm 2$  pmol mol<sup>-1</sup>. However, unlike HFC-23, the annual average HCFC-22 growth rate slowed from 2009 to 2016 at an annual average rate of  $-0.5$  pmol mol<sup>-1</sup> yr<sup>-2</sup>. This slowing atmospheric growth

is consistent with HCFC-22 moving from dispersive (high fractional emissions) to feedstock (low fractional emissions) uses, with HFC-23 emissions remaining as a consequence of incomplete mitigation from all HCFC-22 production.

Our results demonstrate that, following a minimum in HFC-23 global emissions in 2009 of  $9.6 \pm 0.6$ , emissions increased to a maximum in 2014 of  $14.5 \pm 0.6$  Gg yr<sup>-1</sup> and then declined to  $12.7 \pm 0.6$  Gg yr<sup>-1</sup> ( $157$  Mt CO<sub>2</sub> eq. yr<sup>-1</sup>) in 2016. The 2009 emissions minimum is consistent with estimates based on national reports and is likely a response to the implementation of the Clean Development Mechanism (CDM) to mitigate HFC-23 emissions by incineration in developing (non-Annex 1) countries under the Kyoto Protocol. Our derived cumulative emissions of HFC-23 during 2010–2016 were  $89 \pm 2$  Gg ( $1.1 \pm 0.2$  Gt CO<sub>2</sub> eq.), which led to an increase in radiative forcing of  $1.0 \pm 0.1$  mW m<sup>-2</sup> over the same period. Although the CDM had reduced global HFC-23 emissions, it cannot now offset the higher emissions from increasing HCFC-22 production in non-Annex 1 countries, as the CDM was closed to new entrants in 2009. We also find that the cumulative European HFC-23 emissions from 2010 to 2016 were  $\sim 1.3$  Gg, corresponding to just 1.5 % of

cumulative global HFC-23 emissions over this same period. The majority of the increase in global HFC-23 emissions since 2010 is attributed to a delay in the adoption of mitigation technologies, predominantly in China and East Asia. However, a reduction in emissions is anticipated, when the Kigali 2016 amendment to the Montreal Protocol, requiring HCFC and HFC production facilities to introduce destruction of HFC-23, is fully implemented.

## 1 Introduction

Due to concerns about climate change, trifluoromethane ( $\text{CHF}_3$ , HFC-23) has attracted interest as a potent greenhouse gas due to a 100 year integrated global warming potential (GWP) of 12 400 (Myhre et al., 2013) and an atmospheric lifetime of  $\sim 228$  years (SPARC, 2013). Hydrofluorocarbons (HFCs) were introduced as replacements for ozone-depleting chlorofluorocarbons (CFCs) and hydrochlorofluorocarbons (HCFCs) – for example, HFC-134a as a direct replacement for CFC-12 (Xiang et al., 2014). However, HFC-23 is a by-product of chlorodifluoromethane HCFC-22 ( $\text{CHClF}_2$ ) production, resulting from the over-fluorination of chloroform ( $\text{CHCl}_3$ ). Most HFC-23 has historically been vented to the atmosphere (UNEP, 2017a). HFC-23 has also been used as a feedstock in the production of Halon-1301 ( $\text{CBrF}_3$ ; Miller and Batchelor, 2012) which substantially decreased with the phase-out of halons in 2010 under the Montreal Protocol, a landmark international agreement designed to protect the stratospheric ozone layer. HFC-23 also has minor emissive uses in air conditioning, fire extinguishers and semiconductor manufacture (McCulloch and Lindley, 2007) and very minor emissions from aluminium production (Fraser et al., 2013). For developed countries HFC-23 emissions were controlled as part of the “F-basket” under the Kyoto Protocol, an international treaty among industrialised nations that sets mandatory limits on greenhouse gas emissions, ([https://ec.europa.eu/clima/policies/f-gas\\_en](https://ec.europa.eu/clima/policies/f-gas_en)).

In the context of this paper, we discuss “developed” and “developing” countries which we take to be synonymous with Annex 1 (non-Article 5) countries and non-Annex 1 (Article 5) countries, respectively.

There have been a number of previous publications related to HFC-23. Oram et al. (1998) measured HFC-23 by gas chromatography-mass spectrometry (GC-MS) analysis of Cape Grim flask air samples and sub-samples of the Cape Grim Air Archive (CGAA), from 1978 to 1995, and reported a dry-air southern hemispheric atmospheric abundance of  $11 \text{ pmol mol}^{-1}$  in late 1995. Culbertson et al. (2004) estimated global emissions of HFC-23 using a one-box model and GC-MS analysis of North American and Antarctic air samples. A top-down HFC-23 emissions history and a comprehensive bottom-up estimate of global HFC-23 emissions were reported by Miller et al. (2010) using Advanced

Global Atmospheric Gases Experiment (AGAGE) observations (2007–2009) and samples from the CGAA (1978–2009). Montzka et al. (2010), using measurements of firm air from the permeable upper layer of an ice sheet and ambient air collected during three expeditions to Antarctica between 2001 and 2009, constructed a consistent Southern Hemisphere (SH) atmospheric history of HFC-23 that was reasonably consistent with Oram et al. (1998) results. Kim et al. (2010), reported HFC-23 measurements (November 2007–December 2008) from Gosan, Jeju Island and South Korea and also estimated regional atmospheric emissions. Asian emissions of HFC-23, including those for China have been reported by Yokouchi et al. (2006); Stohl et al. (2010); Li et al. (2011); and Yao et al. (2012). Most recently, Fang et al. (2014, 2015) have provided bottom-up and top-down estimates of HFC-23 emissions from China and East Asia and included observed HFC-23 mixing ratios at three stations – Gosan, South Korea, and Hateruma and Cape Ochi-ishi, Japan. Remote sensing observations of HFC-23 in the upper troposphere and lower stratosphere by two solar occultation instruments have also been reported (Harrison et al., 2012), indicating an abundance growth rate of  $5.8 \pm 0.3 \%$  per year, similar to the CGAA surface trend of  $5.7 \pm 0.4 \%$  per year over the same period (1989–2007).

HCFC-22 is used principally in air conditioning and refrigeration, with minor uses in foam blowing and as a chemical feedstock in the manufacture of fluoropolymers, such as polytetrafluorethylene (PTFE). HCFC-22 production and consumption (excluding feedstock use) are controlled under the Montreal Protocol. We have previously reported on the changing trends and emissions of HCFC-22 (Simmonds et al., 2017 and references therein).

Technical solutions to mitigate HFC-23 emissions have included optimisation of the HCFC-22 production process and voluntary and regulatory capture and incineration in developed (Annex 1) countries (McCulloch, 2004). Mitigation in developing countries (non-Annex 1) has been introduced under the United Nations Framework Convention on Climate Change (UNFCCC) Clean Development Mechanism (CDM) to destroy HFC-23 from HCFC-22 production facilities (UNEP, 2017a). This allowed certain HCFC-22 production plants in developing countries to be eligible to provide Certified Emission Reduction (CER) credits for the destruction of the co-produced HFC-23. Beginning in 2003, there were 19 registered HFC-23 incineration projects in five developing countries with the number of projects in each country shown in parenthesis: China (11), India (5), Korea (1), Mexico (1) and Argentina (1) (Miller et al., 2010). The first CER credits under the CDM for HFC-23 abatement in HCFC-22 plants were approved in 2003 with funding through 2009. However, the CDM projects covered only about half of the HCFC-22 production in developing countries. The substantial reduction in global HFC-23 emissions during 2007–2009 was attributed by Miller et al. (2010) to the destruction of HFC-23 by CDM projects. In a subsequent

paper, Miller and Kuijpers (2011) predicted future increases in HFC-23 emissions by considering three scenarios: a reference case with no additional abatement, and two opposing abatement measures, less mitigation and best practice involving increasing application of mitigation through HFC-23 incineration. Historically there has been a lack of information about HFC-23 emissions from the non-CDM HCFC-22 production plants, although Fang et al. (2015) provided a top-down estimate of HFC-23 / HCFC-22 co-production ratios in non-CDM production plants. They reported that the HFC-23 / HCFC-22 co-production ratios in all HCFC-22 production plants were  $2.7\% \pm 0.4$  by mass in 2007, consistent with values reported to the Executive Committee of the Montreal Protocol (UNEP, 2017a).

Here, we use the high-frequency atmospheric observations of HFC-23 and HCFC-22 abundances measured by (GC-MS) at the five longest-running remote sites of the Advanced Global Atmospheric Gases Experiment (AGAGE). The site coordinates and measurement time frames of HFC-23 and HCFC-22 are listed in Table 1. To extend our understanding of the long-term growth rate of HFC-23, we combine the direct AGAGE atmospheric observations with results from an analysis of firn air collected in Antarctica and Greenland, a series of old Northern Hemisphere air samples and archived air from the CGAA (Fraser et al., 1991). The AGAGE 2-D 12-box model and a Bayesian inversion technique are used to produce global emission estimates for HFC-23 and HCFC-22 (Cunnold et al., 1983; Rigby et al., 2011, 2014). We also include observations from the AGAGE Jungfraujoch station to determine estimates of European HFC-23 emissions (see Sect. 3.3).

## 2 Methodology

### 2.1 AGAGE instrumentation and measurement techniques

Ambient air measurements of HFC-23 and HCFC-22 at each site are made using the AGAGE GC-MS-Medusa instrument which employs an adsorbent-filled (HayeSep D) microtrap cooled to  $\sim -175^\circ\text{C}$  to pre-concentrate the analytes during sample collection from 2 L of air (Miller et al., 2008; Arnold et al., 2012). Samples are analysed approximately every 2 h and are bracketed by measurements of quaternary standards to correct for short-term drifts in instrument response. Additional details of the analytical methodology are provided in the Supplement (Sect. S1).

### 2.2 Firn and archived air

We used air samples from firn and archived canisters to reconstruct an atmospheric HFC-23 history. Firn air samples from Antarctica and Greenland were analysed for HFC-23 using the same technology as the in situ measurements; details are provided in the Supplement (Sect. S2). The Antarctic

samples were collected at the DSSW20K Law Dome site in 1997–1998 (Trudinger et al., 2002) and include one deep sample from the South Pole collected in 2001 (Butler et al., 2001). Greenland samples were collected at the NEEM (North Greenland Eemian Ice Drilling) site in 2008 (Buizert et al., 2012). The CSIRO firn model (Trudinger et al., 1997, 2013) was used to derive age spectra for the individual firn samples and more details on these samples and their analysis are given in Vollmer et al. (2016, 2018) and Trudinger et al. (2016). A diffusion coefficient of HFC-23 relative to  $\text{CO}_2$  of 0.797 was used (Fuller et al., 1966).

CGAA measurements from three separate analysis periods were also used for the reconstruction of past HFC-23 abundances. The CGAA samples have been collected since 1978 at the Cape Grim Air Pollution Station and amount to  $> 130$  samples, the majority in internally electropolished stainless steel canisters (Fraser et al., 2016, 2017). Samples were analysed under varying conditions in 2006, 2011 and 2016. Here, we use a composite of the results from these measurement sets. Details are given in the Supplement (Sect. S2) and by Vollmer et al. (2018). A series of old Northern Hemisphere (NH) air samples were also measured together with the measurements of the CGAA samples at the Scripps Institution of Oceanography see Supplement Sect. S2 and Mühle et al. (2010); Vollmer et al. (2016).

### 2.3 Calibration scales

The estimated accuracies of the calibration scales for HFC-23 and HCFC-22 are discussed below and a more detailed discussion of the measurement techniques and calibration procedures are reported elsewhere (Miller et al., 2008; O'Doherty et al., 2009; Mühle et al., 2010). HFC-23 and HCFC-22 measurements from all AGAGE sites are reported relative to the SIO-07 and SIO-05 primary calibration scales respectively, which are defined by suites of standard gases prepared by diluting gravimetrically prepared analyte mixtures in  $\text{N}_2\text{O}$  to near-ambient levels in synthetic air (Prinn et al., 2000; Miller et al., 2008).

The absolute accuracies of these primary standard scales are uncertain because possible systematic effects are difficult to quantify or even identify. Combining known statistical and estimated systematic uncertainties, such as measurement and propagation errors, and quoted reagent purities, generally yields lower uncertainties than are supported by comparisons among independent calibration scales (Hall et al., 2014). Furthermore, some systematic uncertainties may be normally distributed, while others, like reagent purity, are skewed in one direction. Estimates of calibration accuracies and their uncertainties are nevertheless needed for interpretive modelling applications. So, despite the difficulty in estimating unknown uncertainties, it is incumbent on those responsible for the measurements to provide an overall assessment of accuracy. Accordingly, we liberally estimate the absolute accuracies of these measurements as  $-3$  to  $+2\%$  for

**Table 1.** AGAGE sites used in this study, their coordinates and start dates for GC-MS-Medusa measurements of HFC-23 and HCFC-22.

AGAGE site	Latitude	Longitude	HFC-23	HCFC-22
Mace Head (MHD), Ireland*	53.3° N	9.9° W	Oct 2007	Nov 2003
Trinidad Head (THD), California, USA	41.0° N	124.1° W	Sep 2007	Mar 2005
Ragged Point (RPB), Barbados	13.2° N	59.4° W	Aug 2007	May 2005
Cape Matatula (SMO), American Samoa	14.2° S	170.6° W	Oct 2007	May 2006
Cape Grim (CGO), Tasmania, Australia	40.7° S	144.7° E	Nov 2007	Jan 2004
Jungfraujoch, Switzerland*	46.5° N	8.0° E	Apr 2008	Aug 2012
Cape Grim Air Archive			Apr 1978	Apr 1978

\* Observations used for regional European emissions.

HFC-23 and  $\pm 1\%$  for HCFC-22. The larger and asymmetric uncertainty for HFC-23 is due to its lower atmospheric and standard concentration, and to the lower stated purity of the HFC-23 reagent used to prepare the primary calibration scale.

## 2.4 Selection of baseline data (unpolluted background air)

Baseline in situ monthly mean HFC-23 and HCFC-22 mole fractions were calculated by excluding values enhanced by local and regional pollution influences, as identified by the iterative AGAGE pollution identification algorithm (for details, see Appendix in O'Doherty et al., 2001). Briefly, baseline measurements are assumed to have Gaussian distributions around the local baseline value, and an iterative process is used to filter out the data that do not conform to this distribution. A second-order polynomial is fitted to the subset of daily minima in any 121-day period to provide a first estimate of the baseline and seasonal cycle. After subtracting this polynomial from all the observations, a standard deviation and median are calculated for the residual values over the 121-day period. Values exceeding three standard deviations above the baseline are assigned as non-baseline (polluted) and removed from further consideration. The process is repeated iteratively to identify and remove additional non-baseline values until the new and previous calculated median values agree within 0.1 %.

## 2.5 Bottom-up emissions estimates

The sources of information on production and emissions of HFCs are generally incomplete and do not provide a comprehensive database of global emissions. In the Supplement (Sect. S3), we compile global HCFC-22 production and HFC-23 emissions data. HCFC-22 is used in two ways: (1) dispersive applications, such as refrigeration and air conditioning, whose production is controlled under the Montreal Protocol and reported by countries as part of their total HCFC production statistics, and (2) feedstock applications in which HCFC-22 is a reactant in chemical processes to produce other products. Although there is an obligation on coun-

tries to report HCFC-22 feedstock use to UNEP, this information is not made public. HCFC-22 production for dispersive uses was calculated from the UNEP HCFC database (UNEP, 2017b) and the Montreal Protocol Technology and Economic Assessment Panel 2006 Assessment (TEAP, 2006). Production for feedstock use was estimated using trade literature as described in the Supplement (Sect. S3) and the sum of production for dispersive and feedstock uses is shown in Table S3.

HFC-23 emissions from Annex 1 countries are reported as a requirement of the UNFCCC. Table S4 shows the total annual HFC-23 emissions reported by these countries (UNFCCC, 2009). There is a small uncertainty in these UNFCCC emissions due to whether countries report on a calendar or fiscal year basis. The data include emissions from use of HFC-23 in applications such as semiconductor manufacture and fire suppression systems. These minor uses of HFC-23, originally produced in a HCFC-22 plant, will result in the eventual emission of most or all into the atmosphere and emissions have remained relatively constant at  $0.13 \pm 0.01 \text{ Gg yr}^{-1}$ , a maximum of 10 % of all emissions (UNFCCC, 2009). Non-Annex 1 countries listed in Table S4 were eligible for financial support for HFC-23 destruction under the CDM. Their emissions were calculated by applying factors to their estimated production of HCFC-22 and offsetting this by the amount destroyed under CDM, as described in the Supplement (Sect. S3). We discuss these independent emission estimates because they are useful as a priori data constraints ("bottom-up" emission estimates) which we compare to observation-based "top-down" estimates.

## 2.6 Global atmospheric model

Emissions were estimated using a Bayesian approach in which our a priori estimates of the emissions growth rate were adjusted by comparing modelled baseline mole fractions to the atmospheric observations (Rigby et al., 2011, 2014). The firm air measurements were included in the inversion, with the age spectra from the firm model used to relate the firm measurements to high-latitude atmospheric mole fractions (Trudinger et al., 2016; Vollmer et al., 2016). A 12-box model of atmospheric transport and chemistry was

used to simulate baseline mole fractions, which assumed that the atmosphere was divided into four zonal bands (90–30° N, 30–0° N, 0–30° S and 30–90° S) and at 500 and 200 hPa vertically (Cunnold et al., 1994; Rigby et al., 2013). The model uses an annually repeating, monthly varying hydroxyl radical (OH) field from Spivakovsky et al. (2000), which has been adjusted to match the observed trend in methyl chloroform (e.g. Rigby et al., 2013). For the gases in this paper, potential variations in OH concentration (e.g. Rigby et al., 2017) were not found to lead to a large change in the derived emissions (see Sect. S4). Annually repeating, monthly varying transport parameters were used as described in Rigby et al. (2014). The temperature-dependent rate constant for reaction with OH was taken from Burkholder et al. (2015), which led to a lifetime of 237 years for HFC-23 and 11.6 years for HCFC-22. As in previous publications (e.g. Rigby et al., 2014), uncertainties in the monthly mean baseline observations in each semi-hemisphere were taken to be the quadratic sum of the measurement repeatability and the variability of the observations within the month that were flagged as “baseline”, using the method in O’Doherty et al. (2001). The variability was used to approximate model uncertainty, as it was assumed to be a measure of the timescales not resolved by the model. No correlated uncertainties were assumed in the model-measurement mismatch uncertainty and both the model-measurement mismatch and the a priori constraint were assumed to be described by Gaussian probability density functions. Seasonal emissions estimates in each semi-hemisphere were derived in the inversion. The inversion propagates uncertainty estimates from the measurements, model and prior emissions growth rate to these a posteriori emissions estimates. The prior emissions growth rate uncertainty was somewhat arbitrarily chosen at a level of 20 % of the maximum a priori emissions and no correlation was assumed between prior estimates of annual emissions growth rate. In contrast to Rigby et al. (2014), in which a scaling factor of the emissions was solved for in the inversion, here we determined absolute emissions, which were found to lead to more robust uncertainty estimates when emissions were very low. A posteriori emissions uncertainties were augmented with an estimate of the influence of uncertainties in the lifetime, as described in Rigby et al. (2014).

## 2.7 Regional-scale atmospheric inversion

HFC-23 pollution events are still observed at sites in north East Asia and Europe. The former have recently been used in regional-scale inverse modelling studies to derive emission estimates for the Asian region and these results are summarised in Sect. 3.3. In contrast, little attention has recently been given to HFC-23 emissions from Europe. We examine European emissions, using a regional-scale inversion tool based on source sensitivities as estimated by a Lagrangian Particle Dispersion Model run in backward mode, combined with a Bayesian inversion framework.

### 2.7.1 Transport simulations

Surface source sensitivities were computed with the Lagrangian Particle Dispersion Model (LPDM) FLEXPART (Stohl et al., 2005) driven by operational analysis/forecasts from the European Centre for Medium-Range Weather Forecasts (ECMWF) Integrated Forecasting System (IFS) modelling system with a horizontal resolution of  $0.2^\circ \times 0.2^\circ$  for central Europe and  $1^\circ \times 1^\circ$  elsewhere. 50 000 model particles were released for each 3-hourly time interval and followed backward in time for 10 days.

### 2.7.2 Bayesian inversion framework

A spatially resolved, regional-scale emission inversion, using the FLEXPART-derived source sensitivities and a Bayesian approach was applied to estimate European HFC-23 annual emissions for individual years between 2009 and 2016. The details of the inversion method were recently published in estimating Swiss methane emissions (Henne et al., 2016). This inversion methodology was part of an HFC inversion inter-comparison (Brunner et al., 2017) and was applied to HFC and HCFC emissions in the eastern Mediterranean (Schönenberger et al., 2017). Here, the inversion relies on the continuous observations from the Jungfraujoch and Mace Head and requires a priori estimates of the emissions distribution. The observations are split into a baseline concentration and above-baseline excursions of the signal that are attributed to recent emissions using the method of Ruckstuhl et al. (2012). The inversion estimates spatially distributed, annual mean emissions and a 2-weekly concentration baseline. In the case of HFC-23 the baseline concentration is very well defined due to the relatively infrequent occurrence of larger pollution events. The inversion results were not significantly different when the baseline was not updated as part of the inversion. The spatial distribution was solved on a grid with different sized rectangular cells. The grid size was inversely proportional to annual total source sensitivities and, therefore, was finer close to the measurement sites and coarser in more remote regions that seldom influence the sites. In contrast to previous applications, the grid resolution was also increased around likely point emitters in order to better localise these potentially large contributors.

In this study the inversion was set up using complete covariance matrices. We designed the a priori covariance matrix in such a way that the total a priori uncertainty for each of the regions/countries was 200 % and proportional to the emissions in each inversion grid cell. Off-diagonal elements of the matrix were filled with the assumption of exponentially decaying spatial correlation of the uncertainties with a length scale of 10 km. The choice of this rather small spatial correlation scale was motivated by the assumed strong contribution from point source emissions, which should result in spatially rather uncorrelated a priori uncertainties.

The data-mismatch covariance matrix contained uncertainty elements that describe the uncertainty of the observations and the transport model. The observation uncertainty was taken from target gas measurements, whereas the model uncertainty was estimated as the RMSE (root mean square error) of the a priori simulations (Henne et al., 2016). The off-diagonal elements of the covariance matrix were again assumed to exponentially decay with time between the data points. The resulting correlation timescale was estimated separately for each site from a fit to the auto-correlation function of the prior model residuals (see Schönerberger et al., 2017) and was of the order of 0.2 to 0.3 days.

### 2.7.3 A priori emissions and sensitivity inversions

Spatially distributed a priori emissions were generated from individual national inventory reports (NIR) to UNFCCC (2009). Most European countries separately list the emissions of HFC-23 by sector in Table 2(II) of their submissions. Here, we chose two different approaches to spatially distribute these bottom-up estimates and use these as input for two sensitivity inversions. In the first approach (UNFCCC\_org), we directly follow the categorisation in each NIR and assign emissions from “Fluorochemical production” to individual production sites as taken from Keller et al. (2011), and shown in Fig. S4 in the Supplement, whereas emissions from “Electronics industry” and “Product use” were distributed according to population density (Center for International Earth Science Information Network – CIESIN – Columbia University 2016, available at <https://ciesin.columbia.edu/data/hrsl/>). Countries reporting no or zero HFC-23 emissions were assigned a per capita emission factor equal to 1/10 of the average per capita emission factor from reporting countries. This mostly impacts countries at the periphery of the inversion domain. In our second approach (UNFCCC\_r0.5), we used the same spatial disaggregation as before, but assign 50 % of the “Electronics industry” and “Product use” emissions in each country to the likely point source locations and distribute the remainder by population. Inversions using the HFC-23 inventory provided by EDGAR (version 4.2) as a priori were tested. However, these inversions showed much weaker model performance than those based on UNFCCC priors and, hence, were dropped from any further analysis.

## 3 Results and discussion

### 3.1 Atmospheric mole fractions

Figure 1 shows the HFC-23 modelled mole fraction for the four equal-mass latitudinal subdivisions of the global atmosphere calculated from the 12-box model and the combined GC-MS-Medusa in situ measurements (2008–2016), firn air data, old NH air and CGAA data. The lower box shows the annual growth rates. We find that the global modelled

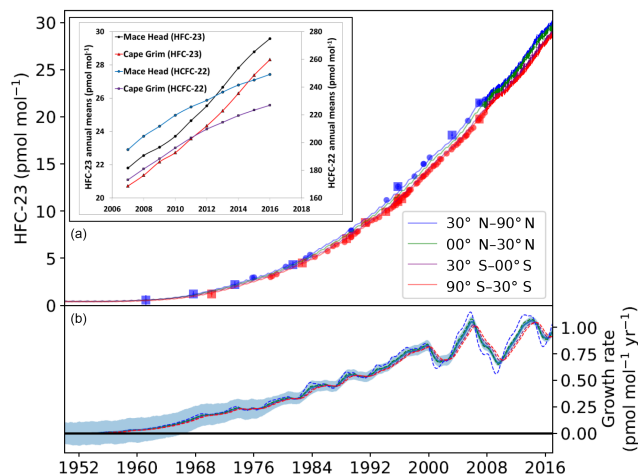


**Figure 1.** (a) HFC-23 modelled mole fractions for the four equal-mass latitudinal subdivisions of the global atmosphere calculated from the 12-box model and the in situ records from the AGAGE core sites (points with error bars), firn air (squares; red SH, blue NH), old NH air data (blue circles, only shown for times without NH in situ data), and CGAA data (red circles, only shown for times without SH in situ data). (b) shows the annual growth rates (global – blue solid line with uncertainty band; and individual semi-hemispheres – dashed lines) in  $\text{pmol mol}^{-1} \text{ yr}^{-1}$ . Figure 1 inset, compares the annual mean mole fractions of HFC-23 and HCFC-22 recorded at Mace Head and Cape Grim from 2007 to 2016.

annual mole fraction of HFC-23 in the background atmosphere reached  $28.9 \pm 0.6 \text{ pmol mol}^{-1}$ , ( $1\sigma$  confidence interval) in December 2016, a 163 % increase from 1995 and a 28 % increase from the  $22.6 \pm 0.2 \text{ pmol mol}^{-1}$  reported in 2009 (Miller et al., 2010). In 2008 the annual mean mid-year growth rate of HFC-23 was  $0.78 \text{ pmol mol}^{-1} \text{ yr}^{-1}$ . By mid-2009 the growth rate decreased to  $0.68 \text{ pmol mol}^{-1} \text{ yr}^{-1}$ , rising to a maximum of  $1.05 \text{ pmol mol}^{-1} \text{ yr}^{-1}$  in early 2014, followed by a smaller decrease to  $0.95 \text{ pmol mol}^{-1} \text{ yr}^{-1}$  in 2016. The growth rate of HFC-23 increased by 22 % from 2008 to 2016. In the Figure 1 inset, we compare the annual mean mole fractions of HFC-23 and HCFC-22 recorded at Mace Head and Cape Grim, as examples of mid-latitude Northern Hemisphere (NH) and Southern Hemisphere (SH) sites, illustrating the site divergence for these two compounds beginning around 2010.

Figure 2 shows our HCFC-22 modelled mole fractions for the four equal-mass latitudinal subdivisions of the global atmosphere calculated from the 12-box model and the lower box shows the HCFC-22 annual growth rates in  $\text{pmol mol}^{-1} \text{ yr}^{-1}$ . The global modelled HCFC-22 annual mixing ratio in the background atmosphere reached peaked at  $238 \pm 2 \text{ pmol mol}^{-1}$  in December 2016, following the decline in the annual average global growth rate of HCFC-22 from 2008 to 2016 of  $0.5 \text{ pmol mol}^{-1} \text{ yr}^{-2}$ . This decline in the global growth rate of HCFC-22 coincides with the phase out of HCFC production/consumption mandated by the 2007



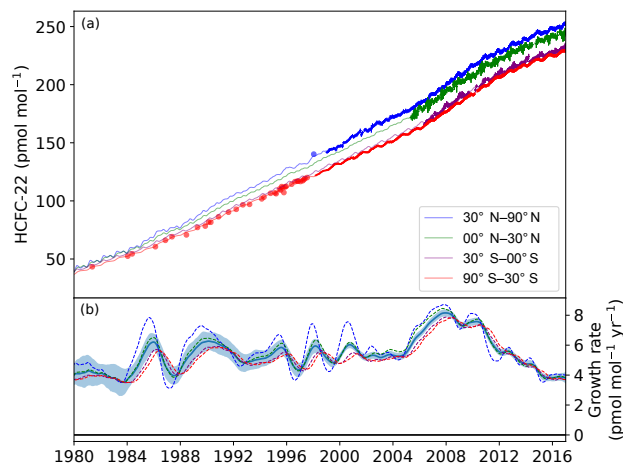


**Figure 2.** (a) HCFC-22 modelled mole fractions for the four equal-mass latitudinal subdivisions of the global atmosphere calculated from the 12-box model and the in situ records from the AGAGE core sites (points with error bars) and CGAA data (red circles, only shown for times without in situ data) and old NH air data (blue circles, only shown for times without NH in situ data). (b) shows the annual growth rates (global – blue solid line with uncertainty band; and individual semi-hemispheres – dashed lines) in  $\text{pmol mol}^{-1} \text{yr}^{-1}$ .

amendment to the Montreal Protocol for Annex 1 countries, covering dispersive applications, but not the non-dispersive use of HCFC-22 as a feedstock in fluoropolymer manufacture (UNEP, 2017a). Nevertheless, HCFC-22 remains the dominant HCFC in the atmosphere and accounts for 79 % by mass of the total global HCFC emissions (Simmonds et al., 2017). In contrast to the increasing growth rate of HFC-23, the growth rate of HCFC-22 has exhibited a steep 53 % decline from a maximum in January 2008 of  $8.2$  to  $3.8 \text{ pmol mol}^{-1} \text{yr}^{-1}$  in December 2016, further illustrating the divergence between these two gases between 2008 and 2016 (compare lower boxes in Figs. 1 and 2). These results are an update of our previously reported analysis AGAGE HCFC-22 data (Simmonds et al., 2017) for the period 1995–2015.

### 3.2 Global emission estimates

Miller et al. (2010) calculated global emissions of HFC-23 using the same AGAGE 12-box model as used here, but with a different Bayesian inverse modelling framework. Following a peak in emissions in 2006 of  $15.9 (+1.3/-1.2) \text{ Gg yr}^{-1}$ , modelled emission estimates of HFC-23 declined rapidly to  $8.6 (+0.9/-1.0) \text{ Gg yr}^{-1}$  in 2009, which Miller noted was the lowest annual emission for the previous 15 years. Based on the analysis of firn air samples and ambient air measurements from Antarctica, Montzka et al. (2010) reported global HFC-23 emissions of  $13.5 \pm 2 \text{ Gg yr}^{-1}$  ( $200 \pm 30 \text{ Mt CO}_2 \text{ eq. yr}^{-1}$ ), averaged over

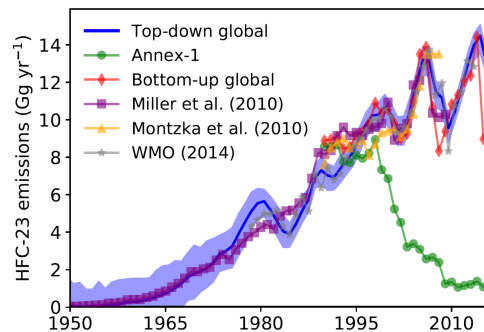


**Figure 3.** Global emissions of HFC-23 calculated from the AGAGE 12-box model (blue line and shading,  $1\sigma$  uncertainty). Data are plotted as annual mean values, centred on the middle of each year. The purple line shows bottom-up HFC-23 estimates of emissions from Miller et al. (2010), the yellow line HFC-23 emissions estimates from Montzka et al. (2010) and the grey line from Carpenter and Reimann (2014). The green line shows emissions reports by Annex-1 countries. The red line shows the bottom-up estimated global emissions developed here and discussed in Sect. S3.

2006–2008. In Carpenter and Reimann (2014), global emissions of HFC-23 estimated from measured and derived atmospheric trends reached a maximum of  $15 \text{ Gg yr}^{-1}$  in 2006, declined to  $8.6 \text{ Gg}$  in 2009, and subsequently increased again to  $12.8 \text{ Gg}$  in 2012 (Figs. 1–25, update of Miller et al., 2010 and Montzka et al., 2010).

The model derived HFC-23 emissions from this study, shown in Fig. 3 and listed in Table 2, reached an initial maximum in 2006 of  $13.3 \pm 0.8 \text{ Gg yr}^{-1}$ , then declined steeply to  $9.6 \pm 0.6 \text{ Gg yr}^{-1}$  in 2009. Our HFC-23 emissions estimates, which include firn data, NH archive air samples and a slightly different inverse method, are slightly lower in 2006 and slightly higher in 2009 than the HFC-23 estimates of Miller et al. (2010) and Carpenter and Reimann (2014) respectively. Our mean annual (2006–2008) HFC-23 emissions of  $12.1 (\pm 0.7) \text{ Gg yr}^{-1}$  are lower than the Montzka et al. (2010) emissions estimates of  $13.5 \pm 2 \text{ Gg yr}^{-1}$ , but agree within uncertainties. However, our HFC-23 emissions then grew rapidly reaching a new maximum of  $14.5 \pm 0.6 \text{ Gg yr}^{-1}$  ( $180 \pm 7 \text{ Mt CO}_2 \text{ eq yr}^{-1}$ ) in 2014, only to decline again to  $12.7 \pm 0.6 \text{ Gg yr}^{-1}$  ( $157 \pm 7 \text{ Mt CO}_2 \text{ eq yr}^{-1}$ ) in 2016. Cumulative HFC-23 emissions estimates from 2010 to 2016 were  $89 \pm 16 \text{ Gg}$  ( $1.1 \pm 0.2 \text{ Gt CO}_2 \text{ eq.}$ ), contributing to an increase in radiative forcing of  $1.0 \pm 0.1 \text{ mW m}^{-2}$ .

The global emission estimates for HCFC-22 are plotted in Figure 4 together with the corresponding Miller et al. (2010) emissions up to 2008 and the WMO 2014 emissions estimates (Carpenter and Reimann, 2014). Table 3 lists the global emission estimates, mole fractions and growth rate of HCFC-22. Our modelled HCFC-22 emissions reached a global maximum of  $385 \pm 41 \text{ Gg yr}^{-1}$  ( $696 \pm 74 \text{ Mt CO}_2 \text{ eq yr}^{-1}$ ) in 2010, followed by a slight



**Table 2.** Annual mean global HFC-23 emissions, mole fractions and growth rates, derived from the AGAGE 12-box model.

Year	HFC-23 global annual emissions (Gg yr <sup>-1</sup> ) ±1 sigma (σ) SD	HFC-23 global mean mole fraction (pmol mol <sup>-1</sup> ) ±1 sigma (σ) SD	HFC-23 global growth rate (pmol mol <sup>-1</sup> yr <sup>-1</sup> ) ±1 sigma (σ) SD
1980	4.2 ± 0.7	3.9 ± 0.1	0.33 ± 0.05
1981	4.2 ± 0.8	4.3 ± 0.1	0.33 ± 0.05
1982	4.4 ± 0.7	4.6 ± 0.1	0.35 ± 0.07
1983	5.2 ± 0.7	5.0 ± 0.1	0.41 ± 0.05
1984	5.6 ± 0.7	5.4 ± 0.1	0.44 ± 0.05
1985	5.8 ± 0.8	5.9 ± 0.1	0.45 ± 0.05
1986	5.8 ± 0.7	6.3 ± 0.1	0.45 ± 0.05
1987	5.9 ± 0.7	6.8 ± 0.1	0.46 ± 0.05
1988	6.8 ± 0.7	7.2 ± 0.1	0.52 ± 0.05
1989	7.1 ± 0.7	7.8 ± 0.2	0.55 ± 0.05
1990	7.0 ± 0.7	8.3 ± 0.2	0.54 ± 0.05
1991	7.0 ± 0.7	8.9 ± 0.2	0.54 ± 0.05
1992	7.4 ± 0.6	9.4 ± 0.2	0.57 ± 0.05
1993	7.9 ± 0.6	10.0 ± 0.2	0.61 ± 0.04
1994	8.3 ± 0.7	10.6 ± 0.2	0.64 ± 0.04
1995	8.9 ± 0.6	11.3 ± 0.2	0.69 ± 0.05
1996	9.6 ± 0.6	12.0 ± 0.2	0.74 ± 0.04
1997	10.1 ± 0.6	12.8 ± 0.3	0.77 ± 0.04
1998	10.4 ± 0.7	13.6 ± 0.3	0.79 ± 0.04
1999	10.9 ± 0.7	14.4 ± 0.3	0.82 ± 0.04
2000	10.4 ± 0.8	15.2 ± 0.3	0.76 ± 0.05
2001	9.4 ± 0.7	15.9 ± 0.3	0.68 ± 0.05
2002	9.5 ± 0.7	16.6 ± 0.3	0.69 ± 0.05
2003	10.3 ± 0.8	17.3 ± 0.3	0.77 ± 0.05
2004	11.8 ± 0.8	18.1 ± 0.3	0.90 ± 0.05
2005	13.2 ± 0.8	19.1 ± 0.4	1.01 ± 0.05
2006	13.3 ± 0.8	20.1 ± 0.4	0.99 ± 0.05
2007	11.7 ± 0.7	21.0 ± 0.4	0.85 ± 0.04
2008	11.2 ± 0.6	21.9 ± 0.4	0.78 ± 0.03
2009	9.6 ± 0.6	22.6 ± 0.4	0.68 ± 0.03
2010	10.4 ± 0.6	23.3 ± 0.4	0.74 ± 0.03
2011	11.6 ± 0.6	24.1 ± 0.5	0.85 ± 0.03
2012	12.9 ± 0.6	25.0 ± 0.5	0.96 ± 0.03
2013	14.0 ± 0.6	26.0 ± 0.5	1.04 ± 0.03
2014	14.5 ± 0.6	27.0 ± 0.5	1.05 ± 0.03
2015	13.1 ± 0.7	28.0 ± 0.5	0.95 ± 0.03
2016	12.7 ± 0.6	28.9 ± 0.6	0.94 ± 0.03

Note: Data are tabulated as annual mean mid-year values. Earlier emissions estimates (1930–1979) determined from the AGAGE 12-box model are listed in the Supplement (Sect. S6), Table S5.

decline to  $370 \pm 46$  Gg yr<sup>-1</sup> ( $670 \pm 83$  Mt CO<sub>2</sub>-eq yr<sup>-1</sup>) in 2016 at an annual average rate of 2.3 Gg yr<sup>-1</sup>.

### 3.3 Regional emissions

Several papers report Asian emissions of HFC-23, including those for China (Yokouchi et al., 2006; Stohl et al., 2010; Kim et al., 2010; Li et al., 2011; Yao et al., 2012). Recent papers by Fang et al. (2014, 2015) noted inconsistencies between the various bottom-up and top-down emissions estimates and provided an improved bottom-up inventory and a multi-annual top-down estimate of HFC-23 emissions for

East Asia. They showed that China contributed 94–98 % of all HFC-23 emissions in East Asia and was the dominant contributor to global emissions:  $20 \pm 6$  in 2000 rising to  $77 \pm 23$  % in 2005. China's annual HFC-23 top-down emissions in 2012 were estimated at  $8.8 \pm 0.8$  Gg yr<sup>-1</sup> (Fang et al., 2015), 69 % of our 2012 global emissions estimate of  $12.9 \pm 0.6$  Gg yr<sup>-1</sup>, listed in Table 2.

Based on the bottom-up estimated global HFC-23 emissions (shown in Sect. S3, Table S4), we show in Fig. 5a global and Chinese emissions and the percentage of Chinese emissions contributing to the global total. These bottom-up

**Table 3.** Annual mean global HCFC-22 emissions, mole fractions, and growth rates, derived from the AGAGE 12-box model.

Year	HCFC-22 global annual emissions (Gg yr <sup>-1</sup> ) ±1 sigma (σ) SD	HCFC-22 global mean mole fraction (pmol mol <sup>-1</sup> ) ±1 sigma (σ) SD	HCFC-22 global growth rate (pmol mol <sup>-1</sup> yr <sup>-1</sup> ) ±1 sigma (σ) SD
1980	116.8 ± 17.6	41.6 ± 1.0	4.1 ± 0.9
1981	123.4 ± 18.8	45.8 ± 1.2	4.2 ± 0.8
1982	125.7 ± 15.7	49.9 ± 1.3	4.0 ± 0.8
1983	125.2 ± 20.1	53.7 ± 0.9	3.6 ± 1.0
1984	136.8 ± 18.1	57.3 ± 1.1	4.2 ± 0.6
1985	166.1 ± 17.0	62.2 ± 1.0	5.7 ± 0.7
1986	174.2 ± 19.3	68.5 ± 1.0	5.5 ± 0.7
1987	155.4 ± 20.2	72.9 ± 1.2	4.1 ± 0.7
1988	177.8 ± 19.6	77.2 ± 1.0	5.0 ± 0.7
1989	198.0 ± 19.8	82.9 ± 1.0	6.0 ± 0.7
1990	209.1 ± 19.7	89.1 ± 1.2	6.2 ± 0.6
1991	212.2 ± 21.4	95.1 ± 1.2	5.8 ± 0.7
1992	207.1 ± 23.9	100.5 ± 1.3	5.0 ± 0.6
1993	214.6 ± 22.8	105.4 ± 1.3	5.0 ± 0.6
1994	222.7 ± 22.9	110.4 ± 1.3	5.2 ± 0.5
1995	241.4 ± 26.9	115.9 ± 1.3	5.7 ± 0.5
1996	230.1 ± 24.3	121.4 ± 1.3	4.8 ± 0.5
1997	238.3 ± 24.1	125.8 ± 1.3	5.0 ± 0.5
1998	256.0 ± 27.2	131.7 ± 1.3	5.7 ± 0.4
1999	251.8 ± 28.4	136.8 ± 1.4	5.0 ± 0.3
2000	275.1 ± 28.7	142.0 ± 1.4	5.8 ± 0.2
2001	275.3 ± 28.8	147.9 ± 1.5	5.5 ± 0.2
2002	280.7 ± 31.6	153.1 ± 1.6	5.3 ± 0.2
2003	286.3 ± 30.1	158.3 ± 1.6	5.3 ± 0.2
2004	292.1 ± 30.6	163.7 ± 1.7	5.3 ± 0.2
2005	312.3 ± 34.6	169.2 ± 1.6	6.1 ± 0.2
2006	334.3 ± 35.0	175.9 ± 1.7	7.2 ± 0.2
2007	355.6 ± 35.2	183.6 ± 1.8	8.0 ± 0.2
2008	372.9 ± 38.4	191.9 ± 1.9	7.9 ± 0.2
2009	368.6 ± 39.7	199.2 ± 2.0	7.4 ± 0.2
2010	385.8 ± 41.3	206.8 ± 2.0	7.4 ± 0.3
2011	373.1 ± 41.3	213.7 ± 2.1	6.2 ± 0.2
2012	373.2 ± 45.5	219.3 ± 2.2	5.5 ± 0.2
2013	369.6 ± 44.1	224.7 ± 2.3	5.0 ± 0.2
2014	373.9 ± 45.7	229.5 ± 2.3	4.6 ± 0.2
2015	364.2 ± 47.7	233.7 ± 2.2	3.9 ± 0.2
2016	370.3 ± 45.9	237.5 ± 2.2	3.9 ± 0.2

Note: Data are tabulated as annual mean mid-year values. These HCFC-22 global emissions estimates are updates of the HCFC-22 emissions reported in Simmonds et al. (2017) for the period 1995–2015.

estimates show that a steadily increasing fraction of global total HFC-23 emissions can be attributed to China, averaging about 88 % in 2011–2014. This rise is consistent with the increase in our calculated bottom-up HCFC-22 production data compiled from industry sources and listed in Sect. S3, Table S3. Figure 5b, shows the bottom-up estimates of global and China HCFC-22 production and the percentage contribution of China production to the global total, further illustrating the dominance of HCFC-22 production in China.

Clearly China is the major contributor to recent global HFC-23 emissions which implies only minor contributions

from other regional emitters. However, HFC-23 pollution events are still observed at our European sites. Keller et al. (2011) reported European HFC-23 emissions based on inverse modelling for the period summer 2008 to summer 2010, assigning most of the emissions to point sources at HCFC-22 production sites. Here, we re-evaluated European HFC-23 emissions for the period 2009 to 2016 (see Sect. 2.7). The key results from this analysis are summarised in Fig. 6 and in Table 4 and more detailed results are available in the Supplement (Sect. S5).

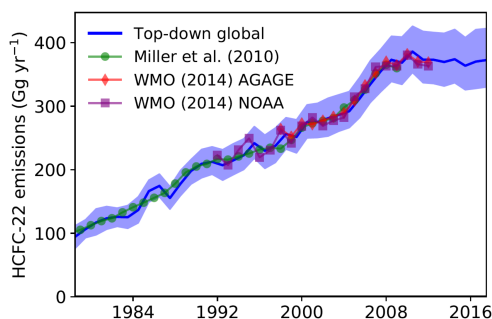
**Table 4.** European HFC-23 emissions (tonne, Mg) by country/region:  $E_a$  a priori,  $E_b$  a posteriori emissions,  $f_a$  fraction of a priori emissions from factory locations,  $f_b$  fraction of a posteriori emissions from factory locations. All values represent averages from both inversions using different a priori distributions.

Year	Germany				France				Italy			
	$E_a$ (Mg yr <sup>-1</sup> )	$E_b$ (Mg yr <sup>-1</sup> )	$f_a$ (%)	$f_b$ (%)	$E_a$ (Mg yr <sup>-1</sup> )	$E_b$ (Mg yr <sup>-1</sup> )	$f_a$ (%)	$f_b$ (%)	$E_a$ (Mg yr <sup>-1</sup> )	$E_b$ (Mg yr <sup>-1</sup> )	$f_a$ (%)	$f_b$ (%)
2009	8 ± 16	34 ± 12	30	49	15 ± 31	2 ± 3.2	88	6	8.4 ± 17	34 ± 8.7	26	52
2010	7.6 ± 15	19 ± 14	27	13	12 ± 23	15 ± 5.1	84	86	9 ± 18	48 ± 9.3	26	45
2011	8 ± 16	44 ± 13	33	58	7.7 ± 15	10 ± 3.4	70	73	9.2 ± 18	34 ± 11	26	43
2012	7.6 ± 15	32 ± 9.7	30	40	8.1 ± 16	8.3 ± 3.4	76	73	9.1 ± 18	25 ± 8.6	26	31
2013	7.2 ± 14	16 ± 9.4	28	58	9.2 ± 18	27 ± 16	82	93	9.3 ± 19	47 ± 24	26	29
2014	7.1 ± 14	20 ± 9.2	30	27	9.4 ± 19	10 ± 2.3	84	85	9.5 ± 19	32 ± 14	26	32
2015	6.6 ± 13	12 ± 8.7	29	14	9.5 ± 19	17 ± 3.9	86	92	9.8 ± 20	37 ± 19	26	24
2016	6.6 ± 13	19 ± 9.1	29	26	9.5 ± 19	9.9 ± 3.4	86	85	9.8 ± 20	23 ± 10	26	39

Year	Benelux				United Kingdom				Iberian Peninsula			
	$E_a$ (Mg yr <sup>-1</sup> )	$E_b$ (Mg yr <sup>-1</sup> )	$f_a$ (%)	$f_b$ (%)	$E_a$ (Mg yr <sup>-1</sup> )	$E_b$ (Mg yr <sup>-1</sup> )	$f_a$ (%)	$f_b$ (%)	$E_a$ (Mg yr <sup>-1</sup> )	$E_b$ (Mg yr <sup>-1</sup> )	$f_a$ (%)	$f_b$ (%)
2009	13 ± 27	25 ± 8.8	98	99	3.8 ± 7.6	5.3 ± 3.1	84	87	97 ± 190	56 ± 29	57	10
2010	34 ± 67	16 ± 7.1	99	98	1.2 ± 2.3	2.8 ± 1.9	48	71	130 ± 260	120 ± 33	66	52
2011	15 ± 29	21 ± 16	97	97	1 ± 2.1	1.5 ± 1.7	39	21	83 ± 170	75 ± 27	50	27
2012	11 ± 22	53 ± 13	96	99	0.92 ± 1.8	2 ± 1.6	26	46	74 ± 150	46 ± 27	45	43
2013	16 ± 33	94 ± 13	98	100	1.1 ± 2.1	2.1 ± 1.8	29	48	64 ± 130	110 ± 27	38	22
2014	3.8 ± 7.6	11 ± 6.3	85	94	1.3 ± 2.5	6.8 ± 2.4	35	73	59 ± 120	55 ± 27	35	45
2015	8.7 ± 17	20 ± 12	94	97	1.4 ± 2.7	2.5 ± 2.1	34	37	48 ± 96	19 ± 18	26	9
2016	8.7 ± 17	45 ± 11	94	99	1.4 ± 2.7	3.8 ± 2.2	34	42	48 ± 96	69 ± 24	26	33

Note: Benelux (Belgium, the Netherlands and Luxembourg).



**Figure 4.** Global emissions of HCFC-22 calculated from the AGAGE 12-box model (blue line and shading,  $1\sigma$  uncertainty). Data are plotted as annual mean mid-year values. The green line shows bottom-up HCFC-22 estimates of emissions from Miller et al. (2010). Red and purple lines show HCFC-22 emissions calculated from AGAGE and NOAA data/models respectively, reported in WMO 2014 (Carpenter and Reimann, 2014).

Based on these inversion results, European emissions of HFC-23, though small on a global scale were, in general, larger than reported to UNFCCC and exhibited considerable year-to-year variability (Table 4, Figs. 6 and S4). Total a posteriori emissions for the six European regions reached

a maximum of  $0.30 \pm 0.05$  Gg yr<sup>-1</sup> in 2013 declining to  $0.17 \pm 0.03$  Gg yr<sup>-1</sup> in 2016 and showed a slightly negative, statistically insignificant trend over the period analysed (2009–2016). The cumulative European HFC-23 emissions from 2010 to 2016 were  $\sim 1.3$  Gg corresponding to just 1.5 % of our cumulative global HFC-23 emissions over this same period of 89 Gg (Table 2). Considerable differences between the two inversions with different a priori emission distributions (see Sect. 2.7.3) were observed on a country scale, with generally larger Italian a posteriori emissions when the original UNFCCC split of point and area sources was used in the a priori (UNFCCC\_org). In this case the inversion was not able to completely relocate the area emissions, but at the same time increased emissions at the point source locations and resulted in overall larger a posteriori emissions. For both sensitivity inversions the fraction of European emissions within grid boxes containing HCFC-22 production facilities, increased in the a posteriori as compared with the a priori distribution (Table 4 and Fig. S4).

In the following section we attempt to reconcile the changing trends in global HFC-23 emissions with the decrease in global HCFC-22 emissions after 2010 and the decline in the annual HCFC-22 growth rate. There are a number of key factors which we believe can explain the changing trend in the

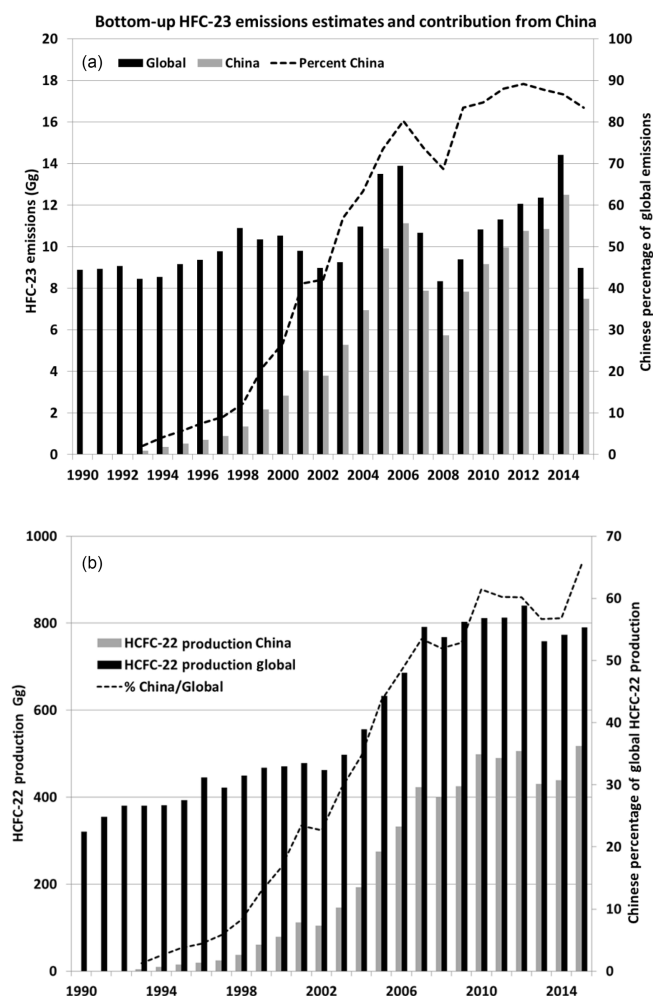


**Figure 5.** (a) HFC-23 global and Chinese emissions estimates and the percentage of Chinese emissions contributing to the global total (dashed line). Compiled from Table S4 in the Supplement. (b) HCFC-22 emissions estimates of global and Chinese production and the percentage of Chinese production as a fraction of the global total (dashed line). Compiled from Table S3.

recent history of HFC-23 emissions after the minimum in 2009.

### 3.4 Factors affecting the recent increase in HFC-23 emissions and changes in the consumption of produced HCFC-22

Recent publications have highlighted the substantial increase in HCFC-22 production in non-Annex 1 countries since the 1990s, especially in the last decade, due to increasing demand in air conditioning, refrigeration applications and primarily from the use of HCFC-22 as a feedstock in fluoropolymer manufacture (UNEP, 2009; Miller et al., 2010; USEPA, 2013; Fang et al., 2015). This has resulted in non-Annex 1 countries emitting more co-produced HFC-23 than Annex 1 countries since about 2001 (Miller et al., 2010). HCFC-

22 production in Annex 1 countries in 2015 had shrunk by 45 % from the peak historic value of  $407 \text{ Gg yr}^{-1}$  in 1996 (see Sect. S3, Table S3). This has been accomplished by plant closures and further reductions of HFC-23 emissions by enhanced destruction in the remaining plants. Nevertheless,  $\sim 1 \text{ Gg}$  of HFC-23 was emitted in 2015 from HCFC-22 production in Annex 1 countries, mainly from Russia and the USA (96 %). For comparison, the combined HFC-23 emissions in 2015 from the six European regions (listed in Table 4) were just  $0.11 \pm 0.03 \text{ Gg}$ .

Since 2006, a major factor mitigating HFC-23 emissions has been the CERs issued under the CDM. However, under the original CDM rules, large CERs that cost relatively little to acquire could be claimed legitimately (Munnings et al., 2016) and the rules were changed to bar new entrants to the mechanism after 2009. The HFC-23 / HCFC-22 co-production or waste gas generation ratio varies between 1.5–4 % (by mass) depending on HCFC-22 plant operating conditions and process optimisation (McCulloch and Lindley, 2007). Under the UNFCCC/CDM, 19 HCFC-22 production plants in five non-Annex 1 countries – Argentina (1), China (11), Democratic People's Republic of Korea (1), India (5) and Mexico (1) – were approved for participation in CDM projects. These countries reportedly incinerated 5.7 and  $6.8 \text{ Gg}$  of HFC-23 in 2007 and 2008, respectively (UNFCCC, 2009). This represented 43–48 % of the HCFC-22 produced in non-Annex 1 countries during 2007–2008 assuming the 1.5–4 % co-production factor (Montzka et al., 2010). These five countries produced  $597 \text{ Gg}$  of HCFC-22 from controlled and feed stock uses in 2015. HFC-23 generated from this HCFC-22 production was estimated at  $16 \text{ Gg}$  with an average co-production ratio of 2.6 %. Furthermore, it was estimated that China produced  $535 \text{ Gg}$  of HCFC-22 in 2015 ( $\sim 90 \%$  of the five countries' total production) and 45 % of the co-produced HFC-23 generated was destroyed in the CDM destruction facilities (UNEP, 2017a). The first seven-year crediting period of CDM projects in China expired in 2013, concurrent with the European Union ceasing the purchase of CER credits for HFC-23 produced in industrial processes after May 2013 (Fang et al., 2014).

Lastly, we should consider whether there are other sources of HFC-23 which might explain an increase in global emissions. While the major source of all HFC-23 is HCFC-22 co-production, material that is recovered and sold may subsequently be emitted to the atmosphere. Emissions of HFC-23 from fire suppression systems are negligible relative to global production (McCulloch and Lindley, 2007) and emissions from all emissive uses are reported to be  $0.13 \pm 0.01 \text{ Gg yr}^{-1}$  from Annex 1 countries (UNFCCC, 2009) and less than  $0.003 \text{ Gg}$  for the refrigeration and fire-fighting sectors in 2015 in the five non-Annex 1 countries listed above, (UNEP, 2017a). Semiconductor use of HFC-23 is insignificant having been replaced by more efficient etchants where destruction efficiencies are greater than 90 % (Bartos et al., 2006; Miller et al., 2010). Fraser et al. (2013) reported a very small emis-

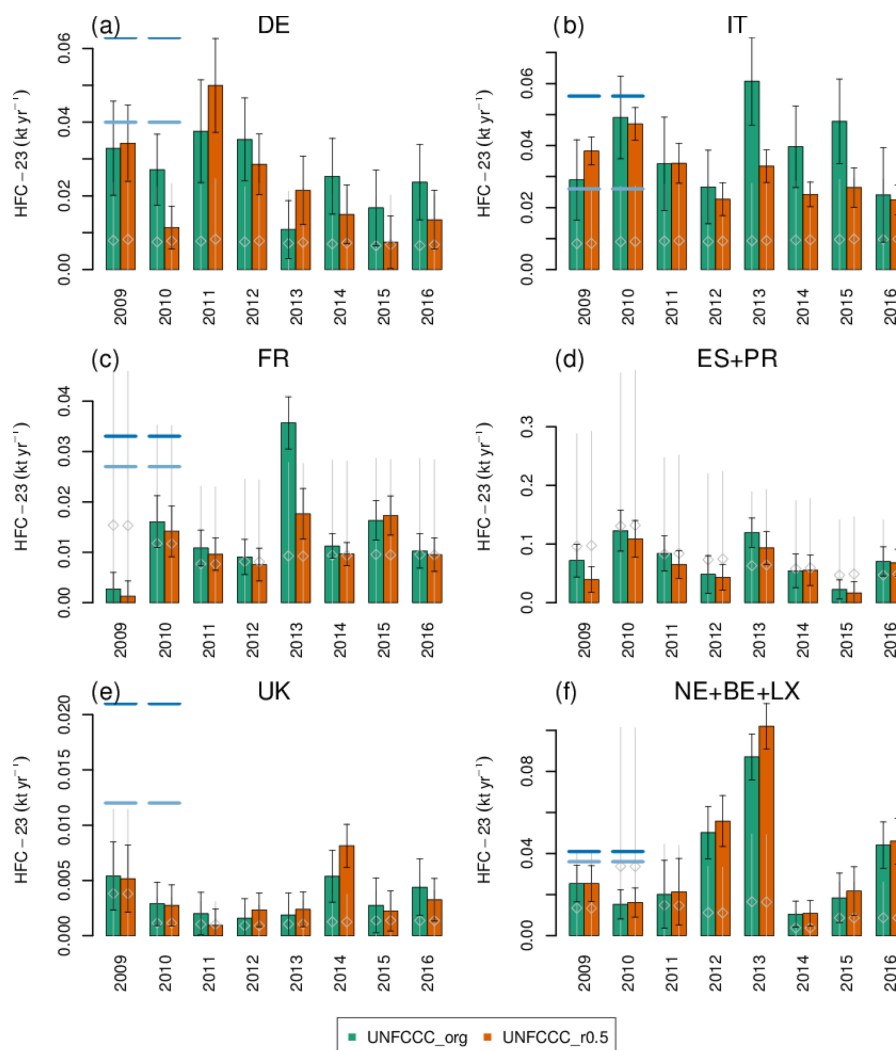


**Figure 6.** Temporal evolution of national/regional emissions of HFC-23: solid bars and error bars give a posteriori emissions using the two sets of a priori emissions (grey lines). The two approaches (green and orange bars) spatially distribute these different bottom-up estimates (see Sect. 2.7.3). Blue horizontal lines give the estimates of Keller et al. (2011) for their Bayesian (light blue) and point source (dark blue) estimate; **(a)** Germany (DE), **(b)** Italy (IT), **(c)** France (FR), **(d)** Spain and Portugal (ES + PR), **(e)** United Kingdom (UK), **(f)** Benelux countries (Netherlands, Belgium and Luxembourg, NE + BE + LX).

sions factor of  $0.04 \text{ g HFC-23 Mg}^{-1}$  aluminium (Al) from the Kurri Kurri smelter in NSW, Australia. It was estimated that this corresponds to an annual emission of HFC-23 from Al production of  $\sim 0.003 \text{ Gg}$  based on a global Al production of  $57 \text{ Tg}$  in 2016 (<http://www.world-aluminium.org/statistics/#data>). Realistically, these other potential industrial sources of HFC-23 emissions are very small ( $< 0.015 \text{ Gg yr}^{-1}$ ) in the context of global emissions estimates.

The combination of these factors strongly suggests that the steep reversal of the downwards trend in HFC-23 emissions after 2009 is attributable to HFC-23 abatement measures not being adequate to offset the increasing growth in production of HCFC-22 for non-dispersive feedstock. This is despite the

initial success of CDM abatement technologies leading to mitigation of HFC-23 emissions during 2006–2009.

## 4 Conclusions

The introduction of CERs under the CDM did contribute to a reduction of HFC-23 emissions in non-Annex 1 countries during 2006–2009, thereby lowering global emissions, reaching a minimum of  $9.6 \pm 0.6 \text{ Gg yr}^{-1}$  in 2009. However, from 2010 to 2014 global HFC-23 emissions increased steadily at an annual average rate of  $\sim 1 \text{ Gg yr}^{-1}$  reaching a new maximum of  $14.5 \pm 0.6 \text{ Gg yr}^{-1}$  in 2014. This period coincides with the highest levels of our bottom-up estimates of HCFC-22 production in non-Annex 1 countries (Sect. S3,

Table S3), coinciding with a transition period when HCFC-22 production plants without any abatement controls had yet to install incineration technologies or fully adopt process optimisation techniques. Furthermore, non-CDM plants are not required to report co-produced HFC-23 emissions, although Fang et al. (2015) calculated that these plants have a lower HFC-23 / HCFC-22 production ratio as they came into operation after the CDM period and would most likely be using improved technologies for HFC-23 abatement.

Our cumulative HFC-23 emissions estimates from 2010 to 2016 were  $89.1 \pm 4.3$  Gg ( $1.1 \pm 0.2$  Gt CO<sub>2</sub>-eq), which led to an increase in radiative forcing of  $1.0 \pm 0.1$  mW m<sup>-2</sup>. This implies that the post-2009 increase in HFC-23 emissions resulted from the decision not to award new CDM projects after 2009, against a background of increasing production of HCFC-22 in plants that did not have abatement technology. Over this same time frame, the magnitude of the cumulative emissions of HCFC-22 was  $2610 \pm 311$  Gg ( $4724$  Mt CO<sub>2</sub>-eq yr<sup>-1</sup>). During 2015–2016 our results show a decline of about 9 % in average global HFC-23 emissions ( $12.9$  Gg yr<sup>-1</sup>) relative to the 2013–2014 average of  $14.2$  Gg yr<sup>-1</sup>. We note that in the Kigali 2016 Amendment to the Montreal Protocol, China committed to a domestic dispersive HCFC-22 production reduction of 10 % by 2015 compared to the average 2009–2010 production (UNEP, 2017a). While this regulation should decrease HCFC-22 production for dispersive uses, overall HFC-23 emissions could still continue to increase due to a potential increase in the production of HCFC-22 for feedstock uses (Fang et al., 2014). It is perhaps encouraging that the Kigali Amendment also stipulates that the Parties to the Montreal Protocol shall ensure that HFC-23 emissions generated from production facilities producing HCFCs or HFCs are destroyed to the maximum extent possible using technology yet to be approved by the Parties. In 2014, with the support of the Chinese Government, 13 new destruction facilities at 15 HCFC-22 production lines not covered by CDM, were installed (UNEP, 2017a). The time frame of these new initiatives is consistent with the most recent reduction (2015–2016) of global HFC-23 emissions.

The mismatch between mitigation and emissions, that is most evident in China, suggests that the delay in the implementation of additional abatement measures allowed HFC-23 emissions to increase before these measures became effective. Our results imply that HFC-23 emissions into the atmosphere will continue to increase and make a contribution to radiative forcing of HFCs until the implementation of abatement becomes a universal requirement.

**Data availability.** The entire ALE/GAGE/AGAGE data base comprising every calibrated measurement including pollution events is archived with the Carbon Dioxide Information and Analysis Center (CDIAC) at the U.S. Department of Energy, Oak Ridge Na-

tional Laboratory (<http://cdiac.ornl.gov>) and also (<http://agage.mit.edu/data/agage-data>).

**The Supplement related to this article is available online at <https://doi.org/10.5194/acp-18-4153-2018-supplement>.**

**Competing interests.** The authors declare that they have no conflict of interest.

**Acknowledgements.** We specifically acknowledge the cooperation and efforts of the station operators (Gerard Spain, Mace Head, Ireland; Randy Dickau, Trinidad Head, California; Peter Sealy, Ragged Point, Barbados; NOAA Officer-in-Charge, Cape Matatula, American Samoa; Sam Cleland, Cape Grim, Tasmania) and their staff at all the AGAGE stations. The operation of the AGAGE stations was supported by the National Aeronautics and Space Administration (NASA, USA; grants NAG5-12669, NNX07AE89G, NNX11AF17G and NNX16AC98G to MIT; grants NAG5-4023, NNX07AE87G, NNX07AF09G, NNX11AF15G, NNX11AF16G, NNX16AC96G and NNX16A97G to SIO). We acknowledge the Department for Business, Energy and Industrial Strategy (BEIS, UK) for contract 1028/06/2015 to the University of Bristol and the UK Meteorological Office in support of Mace Head, Ireland, and modelling activities; the National Oceanic and Atmospheric Administration (NOAA, USA), contract RA-133-R15-CN-0008 to the University of Bristol in support of Ragged Point, Barbados; we acknowledge NOAA support for the operations of the American Samoa station, and support by the Commonwealth Scientific and Industrial Research Organisation (CSIRO, Australia), the Bureau of Meteorology (Australia) and Refrigerant Reclaim Australia for Cape Grim operations.

CSIRO's contribution was supported in part by the Australian Climate Change Science Program (ACCSP), an Australian Government Initiative. Australian firm activities in the Antarctic are specifically supported by the Australian Antarctic Science Program. We acknowledge the members of the firm air sampling teams for provision of the samples from Law Dome, NEEM, and the South Pole. NEEM is directed and organised by the Centre of Ice and Climate at the Niels Bohr Institute and US NSF, Office of Polar Programs. It is supported by funding agencies and institutions in Belgium (FNRS-CFB and FWO), Canada (NRCan/GSC), China (CAS), Denmark (FIST), France (IPEV, CNRS/INSU, CEA, and ANR), Germany (AWI), Iceland (RannIs), Japan (NIPR), Korea (KOPRI), the Netherlands (NWO/ALW), Sweden (VR), Switzerland (SNF), United Kingdom (NERC) and the U.S. (U.S. NSF, Office of Polar Programs). Financial support for the Jungfraujoch measurements is acknowledged from the Swiss national programme HALCLIM (Swiss Federal Office for the Environment (FOEN)). Support for the Jungfraujoch station was provided by International Foundation High Altitude Research Stations Jungfraujoch and Gornergrat (HF-SJG).

Matthew Rigby is supported by a NERC Advanced Fellowship NE/I021365/1. We acknowledge the cooperation of Ray Langenfelds for his long-term involvement in supporting and maintaining



the Cape Grim Air Archive. We also thank Steve Montzka and Brad Hall for supplying actual datasets from their publications.

Edited by: Neil M. Donahue

Reviewed by: two anonymous referees

## References

- Arnold, T., Mühle, J., Salameh, P. K., Harth, C. M., Ivy, D. J., and Weiss, R. F.: Automated measurement of nitrogen trifluoride in ambient air, *Anal. Chem.*, 84, 4798–4804, 2012.
- Bartos, S., Beu, L. S., Burton, C. S., Fraust, C. L., Illuzzi, F., Moccia, M. T., and Raoux, S.: IPCC Guidelines for National Greenhouse Inventories, Vol. 3, Industrial Processes, Chap. 6, Electronics Industry, available at: [www.ipcc-nggip.iges.or.jp/public/2006gl/pdf/3/Volume3/V3.6.Ch6\\_ElectronicsIndustry.pdf](http://www.ipcc-nggip.iges.or.jp/public/2006gl/pdf/3/Volume3/V3.6.Ch6_ElectronicsIndustry.pdf) (last access: 24 August 2017), 2006.
- Brunner, D., Arnold, T., Henne, S., Manning, A., Thompson, R. L., Maione, M., O'Doherty, S., and Reimann, S.: Comparison of four inverse modelling systems applied to the estimation of HFC-125, HFC-134a, and SF<sub>6</sub> emissions over Europe, *Atmos. Chem. Phys.*, 17, 10651–10674, <https://doi.org/10.5194/acp-17-10651-2017>, 2017.
- Burkholder, J. B., Sander, S. P., Abbatt, J., Barker, R., Huie, R. E., Kolb, C. E., Kurylo, M. J., Orkin, V. L., Wilmouth, D. M., and Wine, P. H.: Chemical kinetics and photochemical data for use in atmospheric studies, Evaluation No. 18, JPL Publication 15-10, Jet Propul. Lab., Pasadena, Calif, available at: <http://jpldataeval.jpl.nasa.gov> (last access: 24 August 2017), 2015.
- Buizert, C., Martinerie, P., Petrenko, V. V., Severinghaus, J. P., Trudinger, C. M., Witrant, E., Rosen, J. L., Orsi, A. J., Rubino, M., Etheridge, D. M., Steele, L. P., Hogan, C., Laube, J. C., Sturges, W. T., Levchenko, V. A., Smith, A. M., Levin, I., Conway, T. J., Dlugokencky, E. J., Lang, P. M., Kawamura, K., Jenk, T. M., White, J. W. C., Sowers, T., Schwander, J., and Blunier, T.: Gas transport in firn: multiple-tracer characterisation and model intercomparison for NEEM, Northern Greenland, *Atmos. Chem. Phys.*, 12, 4259–4277, <https://doi.org/10.5194/acp-12-4259-2012>, 2012.
- Butler, J. H., Montzka, S. A., Battle, M., Clarke, A. D., Mondeel, D. J., Lind, J. A., Hall, B. D., and Elkins, J. W.: Collection and analysis of firn air from the South Pole, 2001, AGU Fall Meeting Abstracts, F145, 2001.
- Carpenter, L. J. and Reimann, S.: Ozone-Depleting Substances (ODSs) and Other Gases of Interest to the Montreal Protocol, Chapter 1, in: Scientific Assessment of Ozone Depletion: 2014, Global Ozone Research and Monitoring Project – Report No. 55, World Meteorological Organisation, Geneva, Switzerland, 2014.
- Culberston, J. A., Prins, J. M., Grimsrud, E. P., Rasmussen, R. A., Khalil, M. A. K., and Shearer, M. J.: Observed trends in CF<sub>3</sub>-containing compounds in background air at Cape Meares, Oregon, Point Barrow, Alaska, and Palmer Station, Antarctica, *Chemosphere*, 55, 1109–1119, 2004.
- Cunnold, D. M., Prinn, R. G., Rasmussen, R., Simmonds, P. G., Alyea, F. N., Cardlino, C., Crawford, A. J., Fraser, P. J., and Rosen, R.: The Atmospheric Lifetime Experiment, III: lifetime methodology and application to three years of CFCl<sub>3</sub> data, *J. Geophys. Res.*, 88, 8379–8400, 1983.
- Cunnold, D. M., Fraser, P. J., Weiss, R. F., Prinn, R. G., Simmonds, P. G., Miller, B. R., Alyea, F. N., Crawford, A. J., and Rosen, R.: Global trends and annual releases of CCl<sub>3</sub>F and CCl<sub>2</sub>F<sub>2</sub> estimated from ALE/GAGE and other measurements from July 1978 to June 1991, *J. Geophys. Res.*, 99, 1107–1126, 1994.
- Fang, X., Miller, B. R., Su, S., Wu, J., Zhang, J., and Hu, J.: Historical emissions of HFC-23 (CHF<sub>3</sub>) in China and projections upon policy options by 2050, *Environ. Sci. Technol.*, 48, 4056–4062, 2014.
- Fang, X., Stohl, A., Yokouchi, Y., Kim, J., Li, S., Saito, T., Park, S., and Hu, J.: Multiannual top-down estimate of HFC-23 emissions in east Asia, *Environ. Sci. Technol.*, 49, 4345–4353, 2015.
- Fraser, P. J., Langenfelds, R. L., Derek, N., and Porter, L. W.: Studies in air archiving techniques, in: Baseline Atmospheric Program (Australia) 1989, Department of the Arts, Sport, the Environment, Tourism and Territories, edited by: Wilson, S. R. and Gras, J. L., Bureau of Meteorology and CSIRO Division of Atmospheric Research, Canberra, Australia, 16–29, 1991.
- Fraser, P., Steele, L. P., and Cooksey, M.: PFC and carbon dioxide emissions from an Australian aluminium smelter using time-integrated stack sampling and GC-MS, GC-FID analysis, *Light Metals 2013*, edited by: Sadler, B., Wiley/TMS 2013, 871–876, 2013.
- Fraser, P. J., Steele, L. P., Pearman, G. I., Coram, S., Derek, N., Langenfelds, R. L., and Krummel, P. B.: Non-carbon dioxide greenhouse gases at Cape Grim: a 40 year odyssey, Baseline Atmospheric Program (Australia) History and Recollections, 40th Anniversary Special Edition, edited by: Derek, N., Krummel, P. B., and Cleland, S. J., Bureau of Meteorology/CSIRO Oceans and Atmosphere, ISSN 0155-6959, 45–76, 2016.
- Fraser, P. J., Pearman, G., and Derek, N. I.: CSIRO non-carbon dioxide greenhouse gas research. Part 1: 1975–1990, Historical Records of Australian Science, <https://doi.org/10.1071/HR17016>, 2017.
- Fuller, E. N., Schettler, P. D., and Giddings, J. C.: A new method for prediction of binary gas-phase diffusion coefficients, *Ind. Eng. Chem.*, 30, 19–27, 1966.
- Hall, B. D., Engel, A., Mühle, J., Elkins, J. W., Artuso, F., Atlas, E., Aydin, M., Blake, D., Brunke, E.-G., Chiavarini, S., Fraser, P. J., Happell, J., Krummel, P. B., Levin, I., Loewenstein, M., Maione, M., Montzka, S. A., O'Doherty, S., Reimann, S., Rhoderick, G., Saltzman, E. S., Scheel, H. E., Steele, L. P., Vollmer, M. K., Weiss, R. F., Worthy, D., and Yokouchi, Y.: Results from the International Halocarbons in Air Comparison Experiment (IHALACE), *Atmos. Meas. Tech.*, 7, 469–490, <https://doi.org/10.5194/amt-7-469-2014>, 2014.
- Harrison, J. J., Boone, C. D., Brown, A. T., Allen, N. D. C., Toon, G. C., and Bernath, P. F.: First remote sensing observations of trifluoromethane (HFC-23) in the upper troposphere and lower stratosphere, *J. Geophys. Res.*, 117, D05308, <https://doi.org/10.1029/2011JD016423>, 2012.
- Henne, S., Brunner, D., Oney, B., Leuenberger, M., Eugster, W., Bamberger, I., Meinhardt, F., Steinbacher, M., and Emmenegger, L.: Validation of the Swiss methane emission inventory by atmospheric observations and inverse modelling, *Atmos. Chem. Phys.*, 16, 3683–3710, <https://doi.org/10.5194/acp-16-3683-2016>, 2016.
- Keller, C. A., Brunner, D., Henne, S., Vollmer, M. K., O'Doherty, S., and Reimann, S.: Evidence for under-reported western Euro-

- pean emissions of the potent greenhouse gas HFC-23, *Geophys. Res. Lett.*, 38, L15808, <https://doi.org/10.1029/2011GL047976>, 2011.
- Kim, J., Li, S., Kim, K. R., Stohl, A., Mühle, J., Kim, S. K., Park, M. K., Kang, D. J., Lee, G., Harth, C. M., Salameh, P. K., and Weiss, R. F.: Regional atmospheric emissions determined from measurements at Jeju Island, South Korea: halogenated compounds from China, *Geophys. Res. Lett.*, 37, L12801, <https://doi.org/10.1029/2010GL043263>, 2010.
- Li, S., Kim, J., Kim, K. R., Mühle, J., Kim, S. K., Park, M. K., Stohl, A., Kang, D. J., Arnold, T., Harth, C. M., Salameh, P. K., and Weiss, R. F.: Emissions of halogenated compounds in East Asia determined from measurements at Jeju Island, Korea, *Environ. Sci. Technol.*, 45, 5668–5675, 2011.
- McCulloch, A.: Incineration of HFC-23 Waste Streams for Abatement of Emissions from HCFC-22 Production: A Review of Scientific, Technical and Economic Aspects, commissioned by the UNFCCC secretariat to facilitate the work of the Methodologies Panel of the CDM Executive Board, available at: [http://cdm.unfccc.int/methodologies/Background\\_240305.pdf](http://cdm.unfccc.int/methodologies/Background_240305.pdf) (last access: 24 August 2017), 2004.
- McCulloch, A. and Lindley, A. A.: Global Emissions of HFC-23 estimated to year 2015, *Atmos. Environ.*, 41, 1560–1566, 2007.
- Miller, B. R., Weiss, R. F., Salameh, P. K., Tanhua, T., Grealley, B. R., Mühle, J., and Simmonds, P. G.: Medusa: A sample pre-concentration and GC-MS detector system for in situ measurements of atmospheric trace halocarbons, hydrocarbons and sulphur compounds, *Anal. Chem.*, 80, 1536–1545, 2008.
- Miller, B. R., Rigby, M., Kuijpers, L. J. M., Krummel, P. B., Steele, L. P., Leist, M., Fraser, P. J., McCulloch, A., Harth, C., Salameh, P., Mühle, J., Weiss, R. F., Prinn, R. G., Wang, R. H. J., O'Doherty, S., Grealley, B. R., and Simmonds, P. G.: HFC-23 ( $\text{CHF}_3$ ) emission trend response to HCFC-22 ( $\text{CHClF}_2$ ) production and recent HFC-23 emission abatement measures, *Atmos. Chem. Phys.*, 10, 7875–7890, <https://doi.org/10.5194/acp-10-7875-2010>, 2010.
- Miller, B. R. and Kuijpers, L. J. M.: Projecting future HFC-23 emissions, *Atmos. Chem. Phys.*, 11, 13259–13267, <https://doi.org/10.5194/acp-11-13259-2011>, 2011.
- Miller, M. and Batchelor, T.: Information paper on feedstock uses of ozone-depleting substances, 72 pp., available at: [https://ec.europa.eu/clima/sites/clima/files/ozone/docs/feedstock\\_en.pdf](https://ec.europa.eu/clima/sites/clima/files/ozone/docs/feedstock_en.pdf) (last access: 24 August 2017), 2012.
- Montzka, S. A., Kuijpers, L., Battle, M. O., Aydin, M., Verhulst, K. R., Saltzman, E. S., and Fahey, D. W.: Recent increases in global HFC-23 emissions, *Geophys. Res. Lett.*, 37, L02808, <https://doi.org/10.1029/2009GL041195>, 2010.
- Mühle, J., Ganesan, A. L., Miller, B. R., Salameh, P. K., Harth, C. M., Grealley, B. R., Rigby, M., Porter, L. W., Steele, L. P., Trudinger, C. M., Krummel, P. B., O'Doherty, S., Fraser, P. J., Simmonds, P. G., Prinn, R. G., and Weiss, R. F.: Perfluorocarbons in the global atmosphere: tetrafluoromethane, hexafluoroethane, and octafluoropropane, *Atmos. Chem. Phys.*, 10, 5145–5164, <https://doi.org/10.5194/acp-10-5145-2010>, 2010.
- Munnings, C., Leard, B., and Bento, A.: The net emissions impact of HFC-23 offset projects from the Clean Development Mechanism, Resources for the Future, Discussion Paper 16-01, 2016.
- Myhre, G., Shindell, D., Bréon, F. M., Collins, W., Fuglestad, J., Huang, J., Koch, D., Lamarque, J. F., Lee, D., Mendoza, B., Nakajima, T., Robock, A., Stephens, G., Takemura, T., and Zhang, H.: Anthropogenic and Natural Radiative Forcing, Chapter 8: Climate Change 2013: The Physical Science Basis, in: Contribution of Working Group I to the Fifth Assessment Report of the Intergovernmental Panel on Climate Change, edited by: Stocker, T. F., Qin, D., Plattner, G.-K., Tignor, M., Allen, S. K., Boschung, J., Nauels, A., Xia, Y., Bex, V., and Midgley, P. M., Cambridge University Press, Cambridge, United Kingdom and New York, NY, USA, 659–740, 2013.
- O'Doherty, S., Cunnold, D., Sturrock, G. A., Ryall, D., Derwent, R. G., Wang, R. H. J., Simmonds, P. G., Fraser, P. J., Weiss, R. F., Salameh, P. K., Miller, B. R., and Prinn, R. G.: *In situ* chloroform measurements at AGAGE atmospheric research stations from 1994–1998, *J. Geophys. Res.*, 106, 20429–20444, 2001.
- O'Doherty, S., Cunnold, D. M., Miller, B. R., Mühle, J., McCulloch, A., Simmonds, P. G., Manning, A. J., Reimann, S., Vollmer, M. K., Grealley, B. R., Prinn, R. G., Fraser, P. J., Steele, P., Krummel, P. B., Dunse, B. L., Porter, L. W., Lunder, C. R., Schmidbauer, N., Hermansen, O., Salameh, P. K., Harth, C. M., Wang, R. H. J., and Weiss, R. F.: Global and regional emissions of HFC-125 ( $\text{CHF}_2\text{CF}_3$ ) from in situ and air archive atmospheric observations at AGAGE and SOGE Observatories, *J. Geophys. Res.*, 114, D23304, <https://doi.org/10.1029/2009JD012184>, 2009.
- Oram, D. E., Sturges, W. T., Penkett, S. A., McCulloch, A., and Fraser, P. J.: Growth of fluorocarbon ( $\text{CHF}_3$ , HFC-23) in the background atmosphere, *Geophys. Res. Lett.*, 25, 35–38, 1998.
- Prinn, R. G., Weiss, R. F., Fraser, P. J., Simmonds, P. G., Cunnold, D. M., Alyea, F. N., O'Doherty, S., Salameh, P. K., Miller, B. R., Huang, J., Wang, R. H. J., Hartley, D. E., Harth, C., Steele, L. P., Sturrock, G., Midgley, P. M., and McCulloch, A.: A history of chemically and radiatively important gases in air deduced from ALE/GAGE/AGAGE, *J. Geophys. Res.*, 105, 17751–17792, <https://doi.org/10.1029/2000JD900141>, 2000.
- Rigby, M., Ganesan, A. L., and Prinn, R. G.: Deriving emissions time series from sparse atmospheric mole fractions, *J. Geophys. Res.*, 116, D08306, <https://doi.org/10.1029/2010JD015401>, 2011.
- Rigby, M., Prinn, R. G., O'Doherty, S., Montzka, S. A., McCulloch, A., Harth, C. M., Mühle, J., Salameh, P. K., Weiss, R. F., Young, D., Simmonds, P. G., Hall, B. D., Dutton, G. S., Nance, D., Mondeel, D. J., Elkins, J. W., Krummel, P. B., Steele, L. P., and Fraser, P. J.: Re-evaluation of the lifetimes of the major CFCs and  $\text{CH}_3\text{CCl}_3$  using atmospheric trends, *Atmos. Chem. Phys.*, 13, 2691–2702, <https://doi.org/10.5194/acp-13-2691-2013>, 2013.
- Rigby, M., Prinn, R. G., O'Doherty, S., Miller, B. R., Ivy, D., Mühle, J., Harth, C. M., Salameh, P. K., Arnold, T., Weiss, R. F., Krummel, P. B., Steele, P. L., Fraser, P. J., Young, D., and Simmonds, P. G.: Recent and future trends in synthetic greenhouse gas radiative forcing, *Geophys. Res. Lett.*, 41, 2623–2630, 2014.
- Rigby, M., Montzka, S. A., Prinn, R. G., White, J. W. C., Young, D., O'Doherty, S., Lunt, M. F., Ganesan, A. L., Manning, A. J., Simmonds, P. G., Salameh, P. K., Harth, C. M., Mühle, J., Weiss, R. F., Fraser, P. J., Steele, L. P., Krummel, P. B., McCulloch, A. and Park, S.: Role of atmospheric oxidation in recent methane growth, *P. Natl. Acad. Sci. USA*, 114, 5373–5377, <https://doi.org/10.1073/pnas.1616426114>, 2017.

- Ruckstuhl, A. F., Henne, S., Reimann, S., Steinbacher, M., Vollmer, M. K., O'Doherty, S., Buchmann, B., and Hueglin, C.: Robust extraction of baseline signal of atmospheric trace species using local regression, *Atmos. Meas. Tech.*, 5, 2613–2624, <https://doi.org/10.5194/amt-5-2613-2012>, 2012.
- Schoenenberger, F., Henne, S., Hill, M., Vollmer, M. K., Kouvarakis, G., Mihalopoulos, N., O'Doherty, S., Maione, M., Emmenegger, L., Peter, T., and Reimann, S.: Abundance and Sources of Atmospheric Halocarbons in the Eastern Mediterranean, *Atmos. Chem. Phys. Discuss.*, <https://doi.org/10.5194/acp-2017-451>, in review, 2017.
- Simmonds, P. G., Rigby, M., McCulloch, A., O'Doherty, S., Young, D., Mühle, J., Krummel, P. B., Steele, P., Fraser, P. J., Manning, A. J., Weiss, R. F., Salameh, P. K., Harth, C. M., Wang, R. H. J., and Prinn, R. G.: Changing trends and emissions of hydrochlorofluorocarbons (HCFCs) and their hydrofluorocarbon (HFCs) replacements, *Atmos. Chem. Phys.*, 17, 4641–4655, <https://doi.org/10.5194/acp-17-4641-2017>, 2017.
- SPARC: Report on the Lifetimes of Stratospheric Ozone-Depleting Substances, Their Replacements, and Related Species, edited by: Ko, M., Newman, P., Reimann, S., and Strahan, S., SPARC Report No. 6, WCRP-15/2013, 2013.
- Spivakovsky, C. M., Logan, J. A., Montzka, S. A., Balkanski, Y. J., Foreman-Fowler, M., Jones, D. B. A., Horowitz, L. W., Fusco, A. C., Brenninkmeijer, C. A. M., Prather, M. J., Wofsy, S. C., and McElroy, M. B.: Three-dimensional climatological distribution of tropospheric OH: Update and evaluation, *J. Geophys. Res.*, 105, 8931–8980, 2000.
- Stohl, A., Forster, C., Frank, A., Seibert, P., and Wotawa, G.: Technical note: The Lagrangian particle dispersion model FLEXPART version 6.2, *Atmos. Chem. Phys.*, 5, 2461–2474, <https://doi.org/10.5194/acp-5-2461-2005>, 2005.
- Stohl, A., Kim, J., Li, S., O'Doherty, S., Mühle, J., Salameh, P. K., Saito, T., Vollmer, M. K., Wan, D., Weiss, R. F., Yao, B., Yokouchi, Y., and Zhou, L. X.: Hydrochlorofluorocarbon and hydrofluorocarbon emissions in East Asia determined by inverse modeling, *Atmos. Chem. Phys.*, 10, 3545–3560, <https://doi.org/10.5194/acp-10-3545-2010>, 2010.
- TEAP: Technology and Economic Assessment Panel of the Montreal Protocol, 2006 Assessment Report, United Nations Environment Programme, Nairobi, Kenya, 2006.
- Trudinger, C. M., Enting, I. G., Etheridge, D. M., Francey, R. J., Levchenko, V. A., Steele, L. P., Raynaud, D., and Arnaud, L.: Modelling air movement and bubble trapping in firn, *J. Geophys. Res.*, 102, 6747–6763, <https://doi.org/10.1029/96JD03382>, 1997.
- Trudinger, C. M., Etheridge, D. M., Rayner, P. J., Enting, I. G., Sturrock, G. A., and Langenfelds, R. L.: Reconstructing atmospheric histories from measurements of air composition in firn, *J. Geophys. Res.*, 107, 4780, <https://doi.org/10.1029/2002JD002545>, 2002.
- Trudinger, C. M., Enting, I. G., Rayner, P. J., Etheridge, D. M., Buizert, C., Rubino, M., Krummel, P. B., and Blunier, T.: How well do different tracers constrain the firn diffusivity profile?, *Atmos. Chem. Phys.*, 13, 1485–1510, <https://doi.org/10.5194/acp-13-1485-2013>, 2013.
- Trudinger, C. M., Fraser, P. J., Etheridge, D. M., Sturges, W. T., Vollmer, M. K., Rigby, M., Martinerie, P., Mühle, J., Worton, D. R., Krummel, P. B., Steele, L. P., Miller, B. R., Laube, J., Mani, F. S., Rayner, P. J., Harth, C. M., Witrant, E., Blunier, T., Schwander, J., O'Doherty, S., and Battle, M.: Atmospheric abundance and global emissions of perfluorocarbons CF<sub>4</sub>, C<sub>2</sub>F<sub>6</sub> and C<sub>3</sub>F<sub>8</sub> since 1800 inferred from ice core, firn, air archive and in situ measurements, *Atmos. Chem. Phys.*, 16, 11733–11754, <https://doi.org/10.5194/acp-16-11733-2016>, 2016.
- UNEP: United Nations Environment Programme, HCFC Production Data, available at: [http://ozone.unep.org/Data\\_Access/](http://ozone.unep.org/Data_Access/) (last access: 16 September 2017), U.N. Environ. Programme, Nairobi, 2009.
- UNEP: Key aspects related to HFC-23 by-product control technologies, report reference UNEP/OzL.Pro/ExCom/78/9 of 7 March 2017, U.N. Environ. Prog., Nairobi, Kenya, 2017a.
- UNEP: Production and Consumption of Ozone Depleting Substances under the Montreal Protocol, 1986–2015, United Nations Environment Programme, available at: <http://ozone.unep.org/en/data-reporting/data-centre> (last access: 16 September 2017), 2017b.
- UNFCCC: United Nations Framework Convention on Climate Change, Greenhouse Gas Emissions Data, available at: [http://unfccc.int/ghg\\_data/ghg\\_data\\_unfccc/items/4146.php](http://unfccc.int/ghg_data/ghg_data_unfccc/items/4146.php) (last access: 27 September 2017), U.N. Framework Conv. on Climate Change, Bonn, Germany, 2009.
- USEPA: Global mitigation of non-CO<sub>2</sub> greenhouse gases: 2010–2030, United States Environmental Protection Agency, EPA-430-R-13-011, available at: <http://www.epa.gov/climatechange/EPAactivities/economics/nonco2mitigation.html> Accessed 27/07/2017 (last access: 27 July 2017), 2013.
- Vollmer, M. K., Mühle, J., Trudinger, C. M., Rigby, M., Montzka, S. A., Harth, C. M., Miller, B. R., Henne, S., Krummel, P. B., Hall, B. D., Young, D., Kim, J., Arduini, J., Wenger, A., Yao, B., Reimann, S., O'Doherty, S., Maione, M., Etheridge, D. M., Li, S., Verdonik, D. P., Park, S., Dutton, G., Steele, L. P., Lunder, C. R., Rhee, T. S., Hermansen, O., Schmidbauer, N., Wang, R. H. J., Hill, M., Salameh, P. K., Langenfelds, R. L., Zhou, L., Blunier, T., Schwander, J., Elkins, J. W., Butler, J. H., Simmonds, P. G., Weiss, R. F., Prinn, R. G., and Fraser, P. J.: Atmospheric histories and global emissions of halons H-1211 (CBrClF<sub>2</sub>), H-1301 (CBrF<sub>3</sub>), and H-2402 (CBrF<sub>2</sub>CBrF<sub>2</sub>), *J. Geophys. Res. Atmos.*, 121, 3663–3686, <https://doi.org/10.1002/2015JD024488>, 2016.
- Vollmer, M. K., Young, D., Trudinger, C. M., Mühle, J., Henne, S., Rigby, M., Park, S., Li, S., Guillevis, M., Mitrevski, B., Harth, C. M., Miller, B. R., Reimann, S., Yao, B., Steele, L. P., Wyss, S. A., Lunder, C. R., Arduini, J., McCulloch, A., Wu, S., Rhee, T. S., Wang, R. H. J., Salameh, P. K., Hermansen, O., Hill, M., Langenfelds, R. L., Ivy, D., O'Doherty, S., Krummel, P. B., Maione, M., Etheridge, D. M., Zhou, L., Fraser, P. J., Prinn, R. G., Weiss, R. F., and Simmonds, P. G.: Atmospheric histories and emissions of chlorofluorocarbons CFC-13 (CClF<sub>3</sub>),  $\Sigma$ CFC-114 (C<sub>2</sub>Cl<sub>2</sub>F<sub>4</sub>), and CFC-115 (C<sub>2</sub>ClF<sub>5</sub>), *Atmos. Chem. Phys.*, 18, 979–1002, <https://doi.org/10.5194/acp-18-979-2018>, 2018.
- Xiang, B., Prabir, P. K., Montzka, S. A., Miller, S. M., Elkins, J. W., Moore, F. L., Atlas, E. L., Miller, B. R., Weiss, R. F., Prinn, R. G., and Wofsy, S. C.: Global emissions of refrigerants HCFC-22 and HFC-134a: Unforeseen seasonal contributions, *P. Natl. Acad. Sci. USA*, 111, 17379–17384, <https://doi.org/10.1073/pnas.1417372111>, 2014.

- Yao, B., Vollmer, M. K., Zhou, L. X., Henne, S., Reimann, S., Li, P. C., Wenger, A., and Hill, M.: In-situ measurements of atmospheric hydrofluorocarbons (HFCs) and perfluorocarbons (PFCs) at the Shangdianzi regional background station, China, *Atmos. Chem. Phys.*, 12, 10181–10193, <https://doi.org/10.5194/acp-12-10181-2012>, 2012.
- Yokouchi, Y., Taguchi, S., Saito, T., Tohjima, Y., Tanimoto, H., and Mukai, H.: High frequency measurements of HFCs at a remote site in East Asia and their implications for Chinese emissions, *Geophys. Res. Lett.*, 33, L21814, <https://doi.org/10.1029/2006GL026403>, 2006.